

Evaluation of an MPC Strategy for Motorway Traffic Comprising Connected and Automated Vehicles

Georgia Perraki, Claudio Roncoli, Ioannis Papamichail, and Markos Papageorgiou

Abstract—This paper investigates the effectiveness of a Model Predictive Control (MPC) scheme for motorway traffic involving vehicles equipped with Vehicle Automation and Communication Systems (VACS). A stretch of the motorway A20, which connects Rotterdam to Gouda in the Netherlands, is modeled in a microscopic traffic simulation environment. In order to ensure the reliability of the microscopic simulation outcome, the simulation parameters are tuned with the purpose of replicating realistic traffic conditions. The MPC framework is then applied to the calibrated microscopic simulation model aiming at the mitigation of traffic congestion in the case study motorway. The synergistic control measures for coordinated and integrated traffic control are ramp metering, with the use of conventional traffic lights, vehicle speed control, and lane changing control actions that are enabled with the aid of VACS.

I. INTRODUCTION

In order to overcome the problem of traffic congestion and motorway degradation, several traffic management and control methods have been proposed during the last decades. In addition to the conventional control measures, the development of a variety of Vehicle Automation and Communication Systems (VACS) is expected to play a key role on the design and implementation of traffic control strategies which will properly exploit the capabilities of equipped vehicles. Among the numerous publications addressing integrated motorway traffic control with or without VACS, a few works that are most closely related to the present work are highlighted here below.

In [1] the author proposes the use of intelligent devices in Automated Highway Systems (AHS), where it is assumed that platoons of fully automated vehicles may travel in specifically designed motorways. This complex system is suggested to be controlled via a multi-layer control structure, where the traffic flow control strategies are included in a decentralised link-layer. The problem of lane assignment for AHS taking into account the possibility of semi-automated or fully automated driving has been examined in [2] where a partitioned strategy is chosen, and the problem is formed as an optimization problem solved with a genetic algorithm

with the objective of finding proper partitions. A Model Predictive Control (MPC) approach for AHS was proposed in [3], which takes into account roadside controllers and intelligent vehicles organized in platoons, with dynamic speed limits, on-ramp metering and lane allocation used as control measures. The underlying optimization problem for the MPC scheme is nonlinear and non-convex and involves both continuous and integer variables; hence, its solution may turn out to be computationally expensive for real-time application. More recently, a feedback control scheme for lane-changing control at bottleneck locations has been suggested in [3] and [4], whereby vehicles equipped with VACS are intended to receive and execute lane-changing orders so as to maximize the bottleneck throughput.

Various approaches have been proposed for the problem of optimal coordinated and integrated motorway traffic using conventional control measures. An optimal control problem for coordinated variable speed limit and ramp metering actions with the aim of minimizing the total time spent in the conventional motorway traffic has been presented in [5]. The employed traffic flow model is METANET [6] and an MPC approach is used for the real-time operation. A hierarchical MPC approach is introduced in [7] considering the use of ramp metering in order to regulate the inflow from on-ramps to the motorway mainstream. The test case is the Amsterdam ring-road and the outcome of the application for the cases of local feedback control, ideal open-loop control and MPC hierarchical coordinated control is compared. A potential approach for maximizing bottleneck outflow by combining variable speed limits with coordinated ramp metering has been suggested in [8], where the proposed framework is tested using microscopic simulation and results in significant amelioration of the total time spent in the motorway.

The objective of this paper is the evaluation of an MPC strategy proposed in [9]. The control framework has been tested in [9], using a quite simple network, and the microscopic simulator was set with its default parameters. In the present work, the effectiveness and applicability of the proposed strategy is examined using a complex real infrastructure which is simulated by use of the AIMSUN [10] microscopic traffic simulator, after careful calibration and validation utilizing real traffic data. The calibration and validation processes ensure that the microscopic simulation model is capable of replicating reality under different traffic conditions and confirm that the simulation output is reliable. The core of the control strategy is the convex optimization problem proposed in [11] and considers, as decision variables, actions enabled with the aid of VACS.

G. Perraki, I. Papamichail and M. Papageorgiou are with the Department of Production Engineering and Management, Technical University of Crete, Chania, 73100, Greece. Email addresses: gperraki@isc.tuc.gr, ipapa@dssl.tuc.gr and markos@dssl.tuc.gr.

C. Roncoli is with the Department of Built Environment, School of Engineering, Aalto University, 02150 Espoo, Finland. Email address: claudio.roncoli@aalto.fi.

The research leading to these results has been conducted in the frame of the project TRAMAN21, which has received funding from the European Research Council under the European Union's Seventh Framework Programme (FP/2007-2013)/ERC Grant Agreement n. 321132.

The rest of the paper is organized as follows. Section 2, outlines the optimal control problem and the employed MPC scheme. In Section 3, the case study network is briefly described, as well as the behavioral models and the dynamic scenario used in the microscopic simulation. Then, the calibration process is presented, and the simulated speeds are compared to the real measured speeds in order to demonstrate that the microscopic simulation is capable of replicating reality. In Section 4 the setup of the MPC strategy is specified and the results of the control strategy applied to the calibrated model under the assumption that all vehicles are equipped with VACS are presented. Finally, Section 5 summarizes the main findings of the work.

II. OPTIMAL INTEGRATED TRAFFIC CONTROL FRAMEWORK

The employed control framework is based on a piecewise linear macroscopic traffic flow model with linear constraints which was developed in [12]. This model has been eventually used in [11] for an optimal control problem formulation, that results in control actions performed by vehicles equipped with VACS. The reader may refer to the aforementioned publications for more details concerning the control design rationale, while, for the sake of completeness, the basic concept is reproduced below.

The optimal control problem is cast in an MPC framework with receding horizon, whereby the control actions are optimized for a future time window to mitigate potential discrepancies between the model predictions and the application outcome. In the employed control framework it is considered that a central decision maker computes the solution of the optimization problem within the MPC approach, disaggregates the results, and assigns specific vehicle control tasks.

The multi-lane freeway network is subdivided into segment-lane entities with the index $i = 1, \dots, I$ for segments and $j = 1, \dots, J$ for lanes. Each segment-lane entity is indicated as a cell indexed by (i, j) and the control measures that are employed in the proposed framework for integrated traffic control are the following:

- Ramp Metering (RM): It aims to control the inflow from the on-ramps and to prevent mainline traffic congestion. For the RM application, conventional traffic lights are used to limit the entering flow by defining proper red and green phases.
- Mainstream Traffic Flow Control (MTFC) via Variable Speed Limits (VSL): The use of VSL in order to regulate the motorway mainstream flow is a common traffic measure. In the employed control framework it is assumed that the VACS-equipped vehicles traveling in the network can receive and apply a specific speed limit based on their location.
- Lane Changing Control (LCC): This control measure aims to optimally assign the flows among the lanes of the motorway with the purpose of improving traffic flow efficiency. LCC actions are implemented with a number of lane-changing advises sent and executed by vehicles equipped with intelligent devices.

In order to guarantee an adequate flexibility, it is supposed that each of the aforementioned control actions is updated according to a specific control time step which may be specified based on human-factors and other operational requirements. The control time steps are assumed to be integer multiples of the traffic flow model time step. Specifically, we denote by T the model time step for an optimization horizon indexed by $k = 0, 1, 2, \dots, K$, where the simulation time is $t = kT$. The motorway is discretized in space with the definition of cells (i, j) , and each motorway cell is characterized by the following variables:

- Density $\rho_{i,j}(k)$ [veh/km]: The number of vehicles in cell (i, j) , at time step k , divided by the segment length L_i .
- On-ramp queue $w_{i,j}(k)$ [veh]: The number of vehicles queuing at the on-ramp attached to the motorway at cell (i, j) .
- Longitudinal flow $q_{i,j}(k^Q)$ [veh/h]: The traffic volume leaving segment i and entering segment $i+1$, remaining in lane j , during time interval $(k^Q, k^Q+1]$, where $k^Q = \lceil \frac{kT}{T^Q} \rceil$ and T^Q is the control step for MTFC. This is the control variable regarding MTFC actions that are accomplished via appropriate VSL actions.
- Lateral flow $f_{i,j,\bar{j}}(k^F)$ [veh/h]: The traffic volume moving from lane j to lane $\bar{j} = j \pm 1$, remaining in the same segment, during time interval $(k^F, k^F+1]$, where $k^F = \lceil \frac{kT}{T^F} \rceil$ and T^F is the control step for LCC. This is a control variable that reflects the LCC actions.
- On-ramp flow $r_{i,j}(k^R)$ [veh/h]: The traffic volume entering from the on-ramp located at cell (i, j) , during the time interval $(k^R, k^R+1]$, where $k^R = \lceil \frac{kT}{T^R} \rceil$ and T^R is the control step for RM. This is a control variable with regard to the RM actions.

The conservation of vehicles describes the dynamics of densities $\rho_{i,j}(k)$ [veh/km] for each segment-lane (i, j) , where the off-ramp flow is determined as a percentage of the total flow passing through all the lanes of the segment based on the turning rates $\gamma_{i,j}(k)$:

$$\begin{aligned} \rho_{i,j}(k+1) &= \rho_{i,j}(k) + \frac{T}{L_i} [q_{i-1,j}(k^Q) + r_{i,j}(k^R) \\ &\quad - q_{i,j}(k^Q) - \gamma_{i,j}(k) \sum_{j=1}^J q_{i,j}(k^Q) + f_{i,j+1,j}(k^F) \\ &\quad + f_{i,j-1,j}(k^F) - f_{i,j,j-1}(k^F) - f_{i,j,j+1}(k^F)]. \end{aligned} \quad (1)$$

Equation (2) describes the dynamics of queues formed at the on-ramps due to the applied RM actions, with $d_{i,j}(k)$ being the external demand:

$$w_{i,j}(k+1) = w_{i,j}(k) + T[d_{i,j}(k) - r_{i,j}(k^R)] \quad (2)$$

The modeling approach for longitudinal flows is based on the piecewise-linear fundamental diagram illustrated in Fig. 1, which includes the possibility to reflect the capacity drop phenomenon. The fundamental diagram consists of the demand and the supply parts which determine the flow based on the upstream and downstream density, respectively. The capacity drop phenomenon is modeled with the introduction of a linear function on the demand part that decreases according to the slope w^D in case the density $\rho_{i,j}(k)$ in the

upstream cell exceeds the critical density $\rho_{i,j}^{cr}$. The flow that is allowed to leave a completely congested cell ($\rho_{i,j}(k) = \rho_{i,j}^{jam}$ where $\rho_{i,j}^{jam}$ is the maximum admissible density) is $q_{i,j}^{jam}$, while $q_{i,j}^{max}$ is the capacity flow. Finally, the left-hand side of the demand part of the fundamental diagram is modeled as a piecewise linear function composed by two linear pieces, instead of one single linear function, which leads to more realistic representation of undercritical speed behavior of real traffic flow [13]. Specifically, this approach leads to one constant speed value for undercritical situations, where density does not exceed a threshold density value $\rho_{i,j}^a$ ($\rho_{i,j}(k) < \rho_{i,j}^a$), and a lower speed value while approaching the critical density ($\rho_{i,j}^a < \rho_{i,j}(k) < \rho_{i,j}^{cr}$).

The longitudinal flows are constrained based on the upper and lower bounds determined by the fundamental diagram demonstrated in Fig. 1. Inequalities (3), (4) and (5) represent the demand part, while (6) and (7) represent the supply part of the employed fundamental diagram.

$$q_{i,j}(k) \leq v_{i,j}^{free} \rho_{i,j}(k) \quad (3)$$

$$q_{i,j}(k) \leq \frac{v_{i,j}^{free} \rho_{i,j}^a - q_{i,j}^{max}}{\rho_{i,j}^a - \rho_{i,j}^{cr}} \rho_{i,j}(k) + \frac{q_{i,j}^{max} - v_{i,j}^{free} \rho_{i,j}^{cr}}{\rho_{i,j}^a - \rho_{i,j}^{cr}} \rho_{i,j}^a \quad (4)$$

$$q_{i,j}(k) \leq -\frac{q_{i,j}^{max} - q_{i,j}^{jam}}{\rho_{i,j}^{jam} - \rho_{i,j}^{cr}} \rho_{i,j}(k) + \frac{q_{i,j}^{max} \rho_{i,j}^{jam} - q_{i,j}^{jam} \rho_{i,j}^{cr}}{\rho_{i,j}^{jam} - \rho_{i,j}^{cr}} \quad (5)$$

$$q_{i,j}(k) \leq q_{i+1,j}^{max} \quad (6)$$

$$q_{i,j}(k) \leq -\frac{q_{i+1,j}^{max}}{\rho_{i+1,j}^{jam} - \rho_{i+1,j}^{cr}} \rho_{i+1,j}(k) + \frac{q_{i+1,j}^{max} \rho_{i+1,j}^{jam}}{\rho_{i+1,j}^{jam} - \rho_{i+1,j}^{cr}} \quad (7)$$

Inequality (8) represents the upper-bound for lateral flows, determined by the number of vehicles in the current cell (i, j), while (9) is an upper bound considering the available space in the cell that is receiving the lateral flow. Finally, lateral flows are constrained based on (10) with the introduction of an upper bound value f^{max} in order to avoid unrealistic values that cannot materialize in a real case.

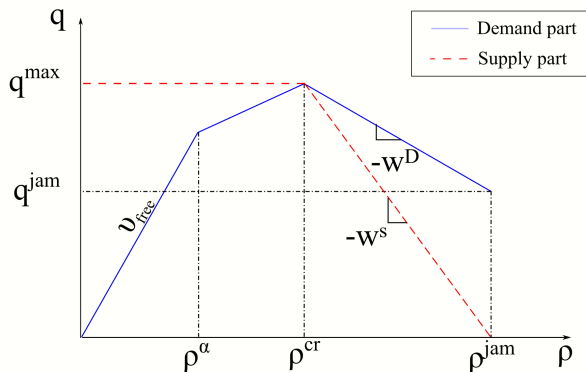


Fig. 1. The proposed FD including both the demand (blue) and the supply (red) piecewise-linear functions.

$$[f_{i,j,j-1}(k^F) + f_{i,j,j+1}(k^F)] \leq \frac{L_i}{T} \rho_{i,j}(k) \quad (8)$$

$$[f_{i,j-1,j}(k^F) + f_{i,j+1,j}(k^F)] \leq \frac{L_i}{T} [\rho_{i,j}^{jam} - \rho_{i,j}(k)] \quad (9)$$

$$\begin{aligned} f_{i,j,j-1}(k^F) &\leq f^{max} \\ f_{i,j,j+1}(k^F) &\leq f^{max} \end{aligned} \quad (10)$$

Fixed upper bounds are also considered for the on-ramp queues and flows i.e. $w_{i,j}(k) < w_{i,j}^{max}$, $r_{i,j}(k^R) < r_{i,j}^{max}$ as well as for the off-ramp flows $\gamma_{i,j}(k) \sum_{j=1}^J q_{i,j}(k^Q) < q_{i,j}^{off,max}$. Finally, non-negativity constraints are specified for all the variables.

The optimization problem is formalized as a convex Quadratic Program (QP), characterized by a convex quadratic cost function subject to constraints (1)-(10). The cost function is composed by two parts, the first part representing the Total Time Spent (TTS) and the second part containing a number of penalty terms.

$$J = J_{TTS} + J_{Penalty} \quad (11)$$

The most important term to be minimized is the TTS that counts the overall time vehicles spent while traveling in the network and queuing at the on-ramps.

$$J_{TTS} = T \sum_{k=1}^K \sum_{i=1}^I \sum_{j=1}^J [L_i \rho_{i,j}(k) + w_{i,j}(k)] \quad (12)$$

The second part of the cost function, $J_{Penalty}$, consists of several penalization terms. In particular, it includes a linear term that aims at penalising excessive lateral flows, and several quadratic penalty terms in order to reduce time variations of RM and LCC control variables as well as to reduce time and space fluctuations of the speed values (approximated via appropriate linearised expressions). Appropriate weight coefficients are utilized for each one of the penalisation terms in order to reflect the respective control priorities.

III. MICROSCOPIC SIMULATION MODEL

A. Network description

The motorway stretch selected for the calibration of the microscopic simulation model and for the application of the MPC scheme, is part of the motorway A20, which connects Rotterdam to Gouda in the Netherlands. The network, which is about 9.3 km in length, is composed by 3 lanes until its 3.6 km where the leftmost lane drops, and it also contains 2 on-ramps and 2 off-ramps as illustrated in Fig. 2. The same case study motorway has been used in [14] and [15].

B. Microscopic simulation behavioral models

AIMSUN microscopic traffic simulator has been employed in order to test the efficiency of the MPC framework. The specific traffic simulation software provides increased flexibility regarding the driver's behavioral models. This is due to its microSDK tool which is used in order to overwrite the default behavioral models. Additionally, the AIMSUN API is exploited for various tasks of the present study.

The Gipps car-following model [16] that is used by default in AIMSUN cannot always reproduce capacity drop phenomena in critical regimes [17]. Hence, it has been replaced in our work with the Intelligent Driver Model (IDM) car-following model [18]. The IDM microscopic model, which can reflect significant aspects of the traffic flow dynamics, shows crash-free collective dynamics and implements an intelligent braking strategy with smooth transitions between acceleration and deceleration behavior [19].

Moreover, the default AIMSUN lane-changing model, which is Gipps [20] lane-changing model, cannot capture the merging behavior in a critical flow regime [21]. Therefore it has been complemented in our work with some heuristic rules that were firstly introduced in [9] at critical network locations, such as the on-ramps merging and the lane drop area. The heuristic rules consist of a set of inequality conditions between the vehicle's current state, and its threshold values. In particular, linear functions of the vehicle's current position determine the threshold values of the three variables of interest i.e. current speed, relative speed with respect to the target-lane vehicles, and available gap in the target lane. The vehicle moves to its target lane once the inequality conditions are jointly satisfied. In the microscopic model, an on-ramp is followed by an acceleration lane, and the drivers entering from the on-ramp need to change lane in order to eventually pass to the mainstream network. In these acceleration lanes, the default lane-changing model is replaced with the heuristic rules so as to achieve realistic driver merging to the main network from an on-ramp. Similarly, the aforementioned rule-based approach is applied to the lane-drop region where the default model may result in unreasonably long queues difficult to be resolved until the end of the simulation. Thus, these rules are applied at the critical on-ramp and lane-drop areas, while in the rest of the motorway, the Gipps lane-changing model is used.

C. Microscopic simulation setup

The available real data consist of speed and flow measurements from several days during years 2009 and 2010. The dataset collected on Wednesday 26-05-2010 is selected for the model calibration while other datasets are used in order to test the validity of the calibrated model. The duration of the simulation is 4 hours, same as the real data measurements duration. Hence, the traffic demand assigned in the simulation scenario is composed by 240 values with one minute duration for each state. The simulation step of the microscopic traffic simulator is set equal to 0.4 s.

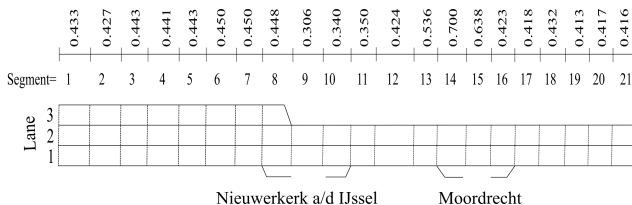


Fig. 2. Stretch of the motorway A20 used as the case study network.

D. Calibration and validation

Firstly, the case study network is cautiously modeled and the dynamic demand scenario is created in the microscopic traffic simulator. Then a sensitivity analysis is conducted in order to define the model parameters that have the biggest impact on the simulation performance. As a result, the parameters to be tuned are maximum acceleration, comfortable deceleration, time headway, desired speed, maximum give-way time and minimum distance.

The calibration of these model parameters is a difficult and tedious task since they have to be calibrated in parallel while taking into account the potential correlation between the parameters of interest. To this end, the calibration procedure is formulated as an optimization problem. Specifically, we use the Root Mean Square Error (RMSE) between the simulated and the observed speeds as the objective function to be minimized and a Genetic Algorithm (GA) is employed to solve this optimization problem. Moreover, it is ensured that the model parameters do not exceed any physical limits by constraining them within assigned lower and upper bounds. Similar approaches that use GA for the calibration of microscopic simulation models can be found in [22] and [23]. After the optimization based parameter setup, the rest of the parameters of the traffic simulator, that have a minor influence on the simulation performance, are manually tuned to achieve an even smaller RMSE value. Regarding the modified lane-changing model, the heuristic lane-changing rules are initially tuned in the acceleration lanes and the lane-drop region based on visual assessment of the resulting vehicle merging behavior while after the simulation parameter setup they are tweaked in the lane-drop section so as to reduce the discrepancies between the queue length formed within the microscopic simulation and the length of the bottleneck appearing in reality.

The left column of Fig. 3 illustrates the speeds observed in the field, while in the right column the speeds produced by the microscopic simulation are displayed. Given that our intention was to replicate the mainline congestion appearing at 06:20 a.m. and there was no interest in reproducing the traffic jams spilling back from the exit of the network, it appears that the microscopic simulation can replicate reality accurately. Congestion is triggered due to the increased demand at the first on-ramp, while the starting time of congestion, its duration and the locations of the bottlenecks appear in very good agreement with reality as well. Finally, the microscopic simulation model is able to reproduce crucial traffic phenomena like the capacity drop (Fig. 5).

The calibrated model is further validated in order to confirm that the microscopic simulation model can replicate real life traffic scenarios under other conditions as well. To this end, different demand profiles are set in the dynamic scenario, based on real data collected on different days, and it is concluded that the microscopic simulation can approach reality under other conditions as well. For the sake of brevity, only the results of the main scenario are presented here, while the validation process results can be found in [24].

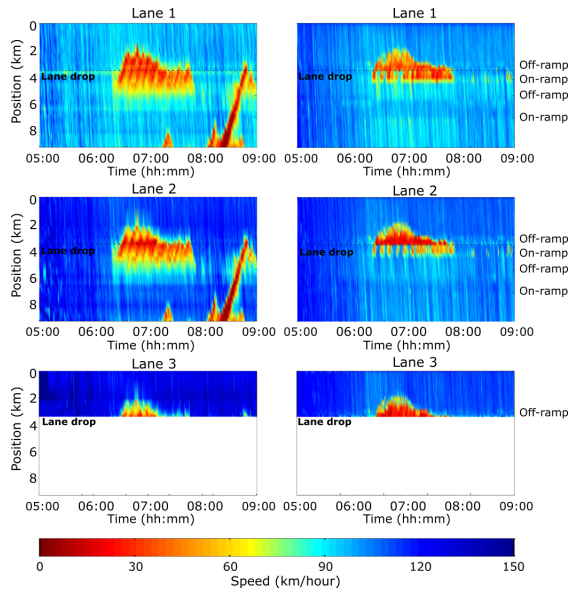


Fig. 3. Contour plots for speeds observed in the field (left column) and produced by the microscopic simulation (right column).

IV. RESULTS

A. MPC problem setup

The case study motorway, which, as described before is about 9.3 km in length, is subdivided in 21 segments with the length of each segment indicated in Fig. 2. Based on this discretization, the control step for the traffic flow model is set to $T = 10$ s, which is the maximum value that satisfies the Courant-Friedrichs-Lewy (CFL) stability condition. A prediction horizon of 10 min is selected for the MPC problem, while the control actions are updated every 1 min based on the latest measurements and predictions. The control steps for RM and LCC actions are set to 1 min whereas a lower time step, equal to the model step, is chosen for the MTFC, i.e. 10 s. The latter has been decided because within the optimization problem the longitudinal flows are constrained by linear functions that depend on the current densities, which are updated according to the model time step. Thus, if the control step for MTFC includes more than one model steps, the longitudinal flow values during the entire control step are upper-bounded by all the constraints defined for each one of the comprised model steps which may cause an unreasonable overconstraining of the computed flow values. However, the control variables of the MTFC actions are eventually averaged according to the update step, i.e. over 1 min, so as to simultaneously apply all the control actions.

For the RM application, traffic lights are placed 10 m upstream of the on-ramp noses aiming at controlling the inflow based on the control variable $r_{i,j}(k^R)$. In the VACS-equipped environment of the application, it is considered that, for the MTFC actions vehicles are receiving and applying specific speed limits according to their current location, while for the LCC actions the optimal lateral flows $f_{i,j,\bar{j}}(k^F)$

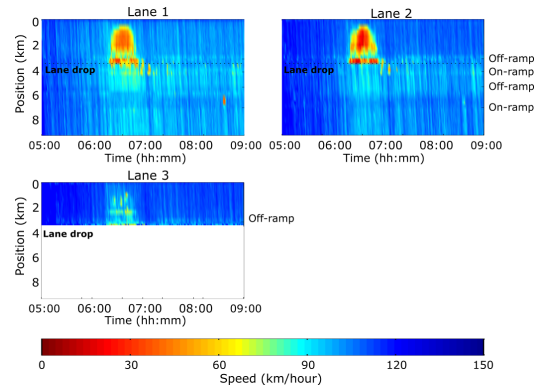


Fig. 4. Speed contour plot in case the MPC scheme is employed in the microscopic simulation.

are translated to a number of lane-changing orders sent to selected VACS-equipped vehicles.

The cost weighting coefficients and the values of the upper and lower bounds on the problem parameters were tuned and kept constant during the simulation. Because of the lane-drop, strong lateral movements are expected from lane 3 to lane 2 of segment 8. Thus, in segment 8-lane 2 we employ a fundamental diagram characterized by a capacity lower than the one utilized in the rest of the network. Note that the possibility to account for a capacity reduction due to the lateral movements is included in the optimization model. However, for the specific application, it was decided, for the sake of simplicity, to refrain from the exploitation of this option, since the capacity of the motorway seemed to remain unaffected by the lateral flow, except for the aforementioned region. Finally, the same dynamic scenario utilized for model calibration is used in order to test the efficiency of the MPC scheme as well. The demand during the rolling optimization horizon is predicted using a naive approach, i.e. set to a constant value equal to the exponentially smoothed value of the past demand.

B. Application results

The no-control case refers to the calibrated microscopic simulation model which as shown in Fig. 3 is capable of sufficiently reproducing real traffic conditions. Fig. 4 displays the measured speeds with the MPC scheme enabled in real-time during the microscopic simulation. Comparing this figure with the right column of Fig. 3, it appears that the duration of the congestion is much less in lanes 1 and 2 while it is almost eliminated in lane 3. As a matter of fact, the emerged small congestion is a consequence of the MTFC actions which aim to achieve capacity flow downstream.

In the no-control case, the TTS value is equal to 1332 veh-h while it drops to 1096 veh-h when the MPC is applied. Hence, a reduction of 17.7% on the TTS is accomplished. Clearly, this percentage is accordingly higher if one restricts the comparison to a tighter space-time window that includes the congestion. This improvement stems mainly from the mitigation of the congestion-induced capacity drop that leads to queue discharge rates lower than the free-flow capacity.

Fig. 5 demonstrates that the throughput during the peak period is increased in the bottleneck location and the motorway is able to operate closer to its nominal capacity thanks to the applied control framework.

The synergistic control actions that lead to the amelioration of the traffic conditions in the motorway are the following:

- Strong LCC actions are performed in segments 6, 7 and 8 in order to move vehicles from lane 3 to the adjacent lane before approaching the lane-drop location. In order to create space in lane 2, sufficient to accommodate the flow entering from lane 3, lateral movements are also requested from lane 2 to lane 1. Fig. 6 displays the computed optimal lateral flows and the actually accomplished right lateral movements from lane 2 to lane 1 in segment 6 with the purpose of creating enough space to lane 2 that is accordingly receiving the illustrated lateral flows from lane 3. As mentioned before, these lateral flows from lane 3 contribute in the mitigation of congestion in the lane-drop area.
- Due to the aforementioned strong LCC actions in segments 6, 7 and 8, the congestion is almost eliminated in lane 3, but the flow arriving in lanes 1 and 2 has to be decreased. This is achieved via MTFC actions from 6:30 AM until 7:00 AM which limit the flow arriving from upstream by the creation of the controlled congestion appearing in Fig. 4. Note however that, the speed through these bottlenecks in lanes 2 and 3 has a higher value than the one in the no-control case.
- The congestion due to the increased demand in Nieuwerkerk aan den IJssel on-ramp is avoided with the application of RM at periods of high demand flow at the on-ramp. At the same time, LCC actions are employed in segment 9 from lane 1 to lane 2, to avoid significant speed breakdown due to the on-ramp merge.
- Small left lateral movements are also requested from lane 1 to lane 2 in segment 15, which is upstream of the segment attached to on-ramp Moordrecht in order to avoid traffic jams at this location. In parallel, RM actions are also applied in periods with high demand at this on-ramp.

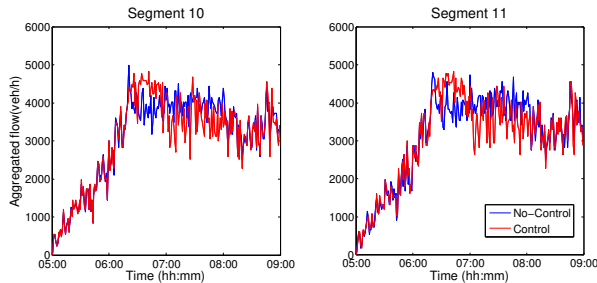


Fig. 5. Comparison between aggregate flows in the control (red) and no-control cases (blue) at segments 10-11.

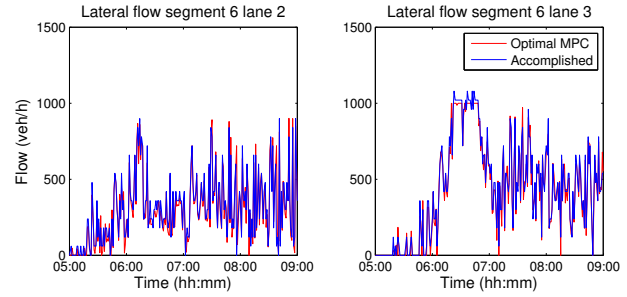


Fig. 6. Comparison between optimal (red) and accomplished (blue) right lateral flows at segment 6.

V. CONCLUSION

An MPC approach, proposed in [9] is extended and tested on a realistic infrastructure using the microscopic traffic simulator AIMSUN, which is initially calibrated in order to reproduce realistic traffic conditions. The test site network is a stretch of the motorway A20 from Rotterdam to Gouda in the Netherlands with two sets of on-off/ramps and a lane-drop. The application of the control strategy on this quite complex infrastructure under realistic traffic conditions demonstrates that the control scheme can mitigate strongly traffic congestion. An improvement of 17.7% on the TTS in the motorway is achieved as a result of the increased throughput due to the MPC application. For the purposes of this paper, the employed control actions are accomplished under the assumption that all vehicles are equipped with VACS, however, another aspect that has to be treated is the consideration of mixed traffic conditions. The introduction of different types of vehicles in the simulated flow, including vehicles equipped with VACS as well as manually driven vehicles, could lead to a more realistic evaluation of the proposed control strategy. Finally, the application of the hierarchical control framework introduced in [25] could also lead to further amelioration of the traffic conditions in the test site motorway.

ACKNOWLEDGMENT

The authors would like to thank Prof. Bart van Arem and his group for their support in providing information related to the network used in the application example.

REFERENCES

- [1] P. Varaiya, "Smart cars on smart roads: problems of control," *IEEE Transactions on Automatic Control*, vol. 38, no. 2, pp. 195–207, 1993.
- [2] K. Kim, J. V. Medani, and D. I. Cho, "Lane assignment problem using a genetic algorithm in the automated highway systems," *International Journal of Automotive Technology*, vol. 9, no. 3, pp. 353–364, 2008.
- [3] C. Roncoli, N. Bekiaris-Liberis, and M. Papageorgiou, "Optimal lane-changing control at motorway bottlenecks," in *Intelligent Transportation Systems (ITSC), 2016 IEEE 19th International Conference on*, 2016, pp. 1785–1791.
- [4] —, "Lane-changing feedback control for efficient lane assignment at motorway bottlenecks," *Transportation Research Record: Journal of the Transportation Research Board*, 2017, to appear.
- [5] A. Hegyi, B. D. Schutter, and H. Hellendoorn, "Model predictive control for optimal coordination of ramp metering and variable speed limits," *Transportation Research Part C: Emerging Technologies*, vol. 13, no. 3, pp. 185–209, 2005.

- [6] A. Messner and M. Papageorgiou, "Metanet: A macroscopic simulation program for motorway networks," *Traffic Engineering & Control*, vol. 31, no. 8-9, pp. 466-470, 1990.
- [7] I. Papamichail, A. Kotsialos, I. Margonis, and M. Papageorgiou, "Coordinated ramp metering for freeway networks a model-predictive hierarchical control approach," *Transportation Research Part C: Emerging Technologies*, vol. 18, no. 3, pp. 311-331, 2010.
- [8] X.-Y. Lu, P. Varaiya, R. Horowitz, D. Su, and S. Shladover, "Novel freeway traffic control with variable speed limit and coordinated ramp metering," *Transportation Research Record: Journal of the Transportation Research Board*, no. 2229, pp. 55-65, 2011.
- [9] C. Roncoli, I. Papamichail, and M. Papageorgiou, "Model predictive control for multi-lane motorways in presence of VACS," in *Proceedings 17th International IEEE Conference on Intelligent Transportation Systems*, 2014, pp. 501-507.
- [10] Transport Simulation Systems, *Aimsun 8 Dynamic Simulators Users' Manual*, Transport Simulation Systems, 2014.
- [11] C. Roncoli, M. Papageorgiou, and I. Papamichail, "Traffic flow optimisation in presence of vehicle automation and communication systems -Part II: Optimal control for multi-lane motorways," *Transportation Research Part C: Emerging Technologies*, vol. 57, pp. 260-275, 2015.
- [12] —, "Traffic flow optimisation in presence of vehicle automation and communication systems - Part I: A first-order multi-lane model for motorway traffic," *Transportation Research Part C: Emerging Technologies*, vol. 57, pp. 241-259, 2015.
- [13] M. Kontorinaki, A. Spiliopoulou, C. Roncoli, and M. Papageorgiou, "Capacity drop in first-order traffic flow models: Overview and real-data validation," in *Transportation Research Board 95th Annual Meeting*, no. 16-3541, 2016.
- [14] W. J. Schakel and B. V. Arem, "Improving traffic flow efficiency by in-car advice on lane, speed, and headway," *IEEE Transactions on Intelligent Transportation Systems*, vol. 15, no. 4, pp. 1597-1606, 2014.
- [15] C. Roncoli, M. Papageorgiou, and I. Papamichail, "Motorway traffic flow optimisation in presence of vehicle automation and communication systems," in *Engineering and Applied Sciences Optimization*. Springer, 2015, pp. 1-16.
- [16] P. Gipps, "A behavioural car-following model for computer simulation," *Transportation Research Part B: Methodological*, vol. 15, no. 2, pp. 105-111, 1981.
- [17] J. Wang, R. Liu, and F. Montgomery, "Car-following model for motorway traffic," *Transportation Research Record: Journal of the Transportation Research Board*, vol. 1934, pp. 33-42, 2005.
- [18] M. Treiber, A. Hennecke, and D. Helbing, "Congested traffic states in empirical observations and microscopic simulations," *Physical Review E*, vol. 62, no. 2, pp. 1805-1824, 2000.
- [19] A. Kesting, M. Treiber, and D. Helbing, "Enhanced intelligent driver model to access the impact of driving strategies on traffic capacity," *Philosophical Transactions of the Royal Society A: Mathematical, Physical and Engineering Sciences*, vol. 368, no. 1928, pp. 4585-4605, Jun 2010.
- [20] P. Gipps, "A model for the structure of lane-changing decisions," *Transportation Research Part B: Methodological*, vol. 20, no. 5, pp. 403-414, 1986.
- [21] E. Chevallier and L. Leclercq, "Do microscopic merging models reproduce the observed priority sharing ratio in congestion?" *Transportation Research Part C: Emerging Technologies*, vol. 17, no. 3, pp. 328-336, 2009.
- [22] R.-L. Cheu, X. Jin, K.-C. Ng, Y.-L. Ng, and D. Srinivasan, "Calibration of fresim for singapore expressway using genetic algorithm," *Journal of Transportation Engineering*, vol. 124, no. 6, pp. 526-535, 1998.
- [23] B. Park and H. Qi, "Microscopic simulation model calibration and validation for freeway work zone network-a case study of vissim," in *Intelligent Transportation Systems Conference, 2006. ITSC'06. IEEE*, 2006, pp. 1471-1476.
- [24] G. Perraki, "Evaluation of a model predictive control strategy on a calibrated multilane microscopic model," Master's thesis, School of Production Engineering and Management, Technical University of Crete, 2016.
- [25] C. Roncoli, I. Papamichail, and M. Papageorgiou, "Hierarchical model predictive control for multi-lane motorways in presence of vehicle automation and communication systems," *Transportation Research Part C: Emerging Technologies*, vol. 62, pp. 117-132, 2016.